

Formation of Thermal Decomposition Cavities in Physical Vapor Transport of Silicon Carbide

EDWARD K. SANCHEZ,¹ THOMAS KUHR,¹ VOLKER D. HEYDEMANN,²
DAVID W. SNYDER,² GREGORY S. ROHRER,¹
and MAREK SKOWRONSKI^{1,3}

1.—Carnegie Mellon University, Department of Materials Science and Engineering, Pittsburgh, PA 15213-3890. 2.—II-VI Incorporated, Saxonburg, PA 16056. 3.—e-mail ms3s@andrew.cmu.edu

The relationship between seed mounting and the formation of thermal decomposition cavities in physical vapor transport grown silicon carbide was investigated. Scanning electron microscopy, energy dispersive x-ray spectroscopy, Auger electron spectroscopy, and optical microscopy were used to characterize thermal decomposition cavities at various stages of their development. The observations indicate that the attachment layer that holds the seed to the graphite crucible lid frequently contains voids. The seed locally decomposes at void locations and Si-bearing species are transported through the void. The decomposition produces a cavity in the seed; the silicon is deposited on and diffuses into the graphite lid. The formation of thermal decomposition cavities can be suppressed by the application of a diffusion barrier on the seed crystal backside.

Key words: Silicon carbide, physical vapor transport, macrodefect, thermal decomposition cavities, seed mounting

INTRODUCTION

Filamentary voids propagating along the *c*-axis of silicon carbide (SiC) single crystals commonly form during physical vapor transport (PVT) growth.¹⁻⁴ These defects intersect the surface of (0001) oriented wafers sliced from such boules and limit the usable area of the substrate. This is problematic for the fabrication of large surface area devices intended for high voltage/high current applications. For example, while the typical pore density in a commercially available wafer is on the order of 10^2 cm⁻², a SiC megawatt device requires a defect free area on the order of 0.4 cm². A review of the literature concerning these voids can be confusing because of the range of terms used for their description. Based on a comparison of the existing literature and our own observations, we believe that it is appropriate to consider two separate classes of voids that have distinct natures and origins. We reserve the commonly used term “micropipe” for the description of approximately cylindrical voids with diameters in the range of 0.1 μ m to 5 μ m that form at the core of super screw dislocations aligned parallel or nearly parallel to the [0001] axis. We refer to larger

voids with diameters from 5 μ m to 100 μ m as “thermal decomposition cavities.”⁵⁻⁷ As an illustration of this difference, Figure 1 shows an optical micrograph of a cross-section of a PVT crystal containing both types of voids.

While the clearest characteristic that distinguishes micropipes and thermal decomposition cavities is their size, the taxonomy we apply here is based on their distinct properties. For example, Stein⁵ demonstrated that the larger thermal decomposition cavities are not replicated in overgrown layers. It has also been shown that tubular voids in SiC wafers can be overgrown by thick epitaxial layers⁸ and that they usually end abruptly in the crystal at plate-like inclusions or voids.⁷ Micropipes, on the other hand, propagate during successive growth steps from the seed to the overgrown layer.⁹ Considering the fact that micropipes are associated with dislocations, this propagation is almost inevitable.¹⁰ Any connection between thermal decomposition cavities and dislocations has yet to be demonstrated; the fact that thermal decomposition cavities can be overgrown suggests that they do not contain super dislocations. Several authors have noted that thermal decomposition cavities originate at the interface between the SiC seed and the graphite seed holder.^{4,7,8} Vodakov et al.⁷ proposed that

(Received August 4, 1999; accepted November 11, 1999)

thermal decomposition cavities form by a recrystallization process in which SiC is transported across small gaps or liquid droplets at the holder/SiC interface. Similarly, Anikin et al.⁸ suggested that they form by localized sublimation from the back of the relatively hot seed to a relatively cool graphite seed holder. In contrast, micropipe initiation has been observed at other points within the crystal, such as second phase precipitates.^{11,12}

Most authors agree that voids in the carbonized sucrose attachment layer at the seed crystal/crucible lid interface create thermal decomposition cavities.^{5,7,8,13} This paper has two objectives. The first is to describe the mechanism by which voids in the attachment layer create thermal decomposition cavities. The second objective is to demonstrate that thermal decomposition cavity formation can be suppressed by controlling the homogeneity of the attachment layer.

EXPERIMENTAL

Crystal Growth

All of the growth experiments were seeded with on-axis (0001) 6H-SiC plates, with lateral dimensions on

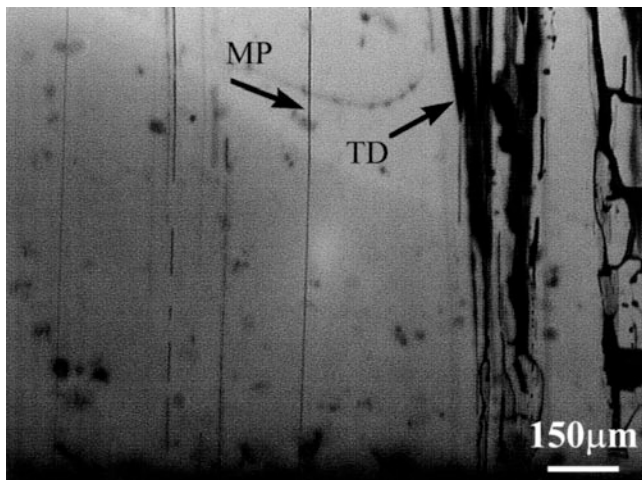


Fig. 1. A transmission optical micrograph of a cross-section slice, parallel to the [0001] growth direction, taken from a 6H SiC boule. The arrows indicate a micropipe (MP) and thermal decomposition cavity (TD).

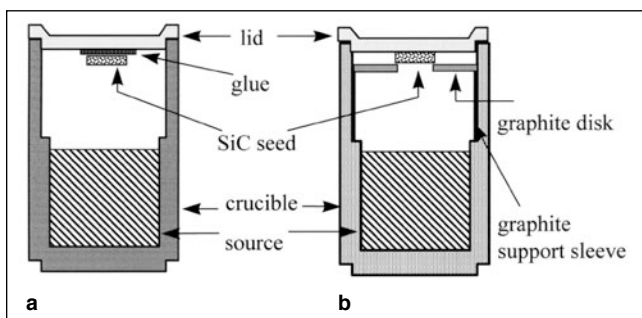


Fig. 2. Schematic diagram of the hot zone used for physical vapor transport growth of SiC. (a) Sucrose mounting method: the seed crystal is attached to the crucible lid with a carbonized sucrose "glue" layer, (b) Mechanical mounting method: the seed crystal is pressed against the crucible lid using a mechanical support disc with a central bore.

the order of 10 mm and a thickness of less than 1 mm. The seed crystals were produced by the Lely method.¹⁴ A wet oxidation treatment ($1100 \pm 50^\circ\text{C}$, for 2–4 h, in H_2O saturated O_2) was used to determine the surface polarity and to clean the surface. Prior to growth, HF was used to strip the oxide layer from the seed surface.

The growth experiments were carried out using a PVT growth apparatus similar to those described in the literature² at either Carnegie Mellon University or II-VI Incorporated. The seed crystal and the SiC charge material were enclosed in a thin walled graphite crucible that was surrounded by an inductively heated graphite susceptor. Both were enveloped by carbon foam insulation and the assembly was contained in an argon filled, water cooled quartz tube. The seed was mounted on the inside surface of the crucible lid. The charge material (1–2 mm grain size high purity Acheson powder produced by Elektroschmelzwerk Delfzijl, Netherlands) was placed in the bottom of the crucible. Optical paths through the insulation allowed the temperature at the top and the bottom of the crucible to be measured by two-color pyrometers.

Two different methods were used for mounting the seed crystals to the graphite lid (see Fig. 2): attachment with carbonized sucrose and mechanical mounting. For the sucrose mounting technique, sucrose is melted on the graphite crucible lid at a temperature of 200°C . The Lely seed is placed on top of the melted sucrose, and a small force is applied to the seed as the melted sucrose graphitizes. The attachment layer is baked to 400°C while the seed is still loaded with a small force. The carbonized attachment layer establishes a rigid bond between the seed and lid. After mounting, the lid and the attachment layer are outgassed under a high vacuum, below 3×10^{-7} torr, in the PVT system at room temperature and then heated in steps to 1200°C . The second method involved pressing the seed crystal against the lid mechanically by the use of a graphite disk and support sleeve.

During each growth run, the hot zone elements (as

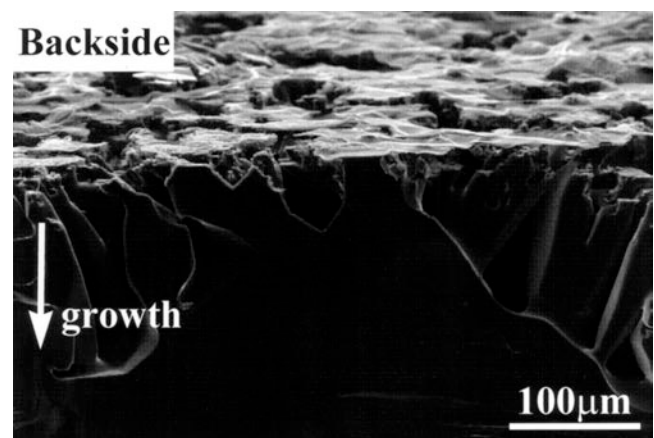


Fig. 3. Scanning electron microscopy (SEM) image of a seed crystal after growth, cleaved along the [0001] axis, perpendicular to the growth surface. The seed crystal was attached to the lid and grown on for an hour at 2300°C and 10 torr. The sample is tilted to exhibit both the cleaved surface and the backside of the seed crystal.

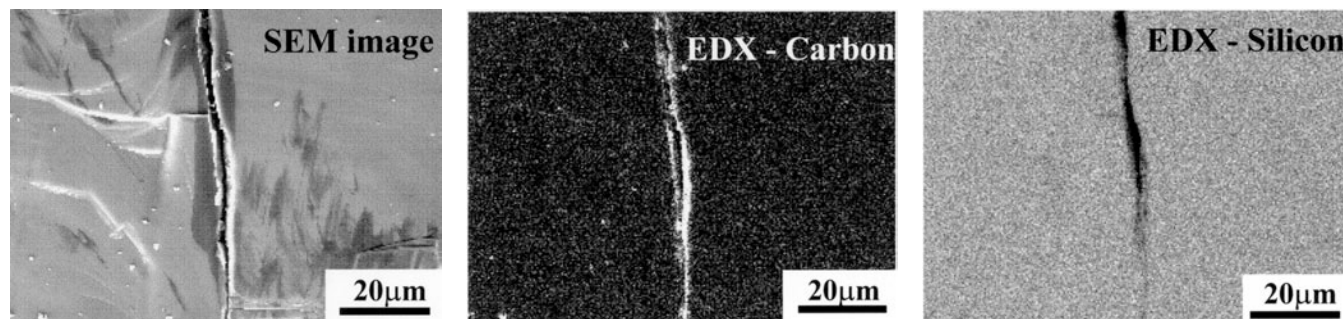


Fig. 4. Secondary electron and energy dispersive x-ray micrographs showing the cross-section of a thermal decomposition cavity in a 6H SiC crystal grown by physical vapor transport. The EDX images show contrast in areas where silicon or carbon is present. The walls of the thermal decomposition cavity are lined with carbon.

seen in Fig. 2) are placed in the PVT system. The system is evacuated to a pressure below 3×10^{-7} torr, then heated in stages to about 1200°C and held for 10 min or until the pressure is reduced below 1×10^{-4} torr. The system is then backfilled with ultra high purity argon to a pressure of 650 torr. The temperature is gradually increased to the growth temperature, 2300°C , at a rate of $24^{\circ}\text{C}/\text{min}$. The duration of individual growth experiments ranged from 15 min to 14 h. During the short runs, the pressure in the growth chamber was maintained at 650 torr to minimize transport of the vapor species, resulting in slow growth rates of approximately 0.05 mm/h. For longer growth runs the argon pressure is reduced to the final growth pressure of 10 to 20 torr. The growth rates observed at reduced pressure were between 0.2 mm/h and 6 mm/h.

Characterization

Scanning electron microscopy (SEM) and energy dispersive x-ray (EDX) images were obtained on a Philips XL-30 microscope under an accelerating voltage of 25 kV. Auger Electron Spectroscopy (AES) was performed on a Physical Electron 600 scanning auger spectrometer under an accelerating voltage of 3 kV. Samples for EDX and AES were cleaved open in order to avoid chemical contamination due to cutting and polishing. Axial slices from PVT grown SiC were obtained for optical transmission images by cutting boules along the *c*-axis with a diamond saw and polishing with diamond paste (down to a particle size of $0.25 \mu\text{m}$).

RESULTS AND DISCUSSION

A single crystal Lely platelet, with flat (0001) surfaces, was attached to a graphite crucible lid using the sucrose attachment method. It was annealed using the growth parameters (2300°C , gradient of $10^{\circ}\text{C}/\text{cm}$, argon pressure of 650 torr) for 15 min and cleaved along the growth direction. The resulting microstructure of the backside and bulk of the seed is shown in the SEM image in Fig. 3. The sample has been tilted to reveal both the backside and cleaved surface of the seed. This figure clearly shows that the seed backside is no longer flat, but contains numerous cavities. These cavities propagate into the crystal along the growth direction, and are visible as they intersect the cleavage plane. It is shown below that these cavities

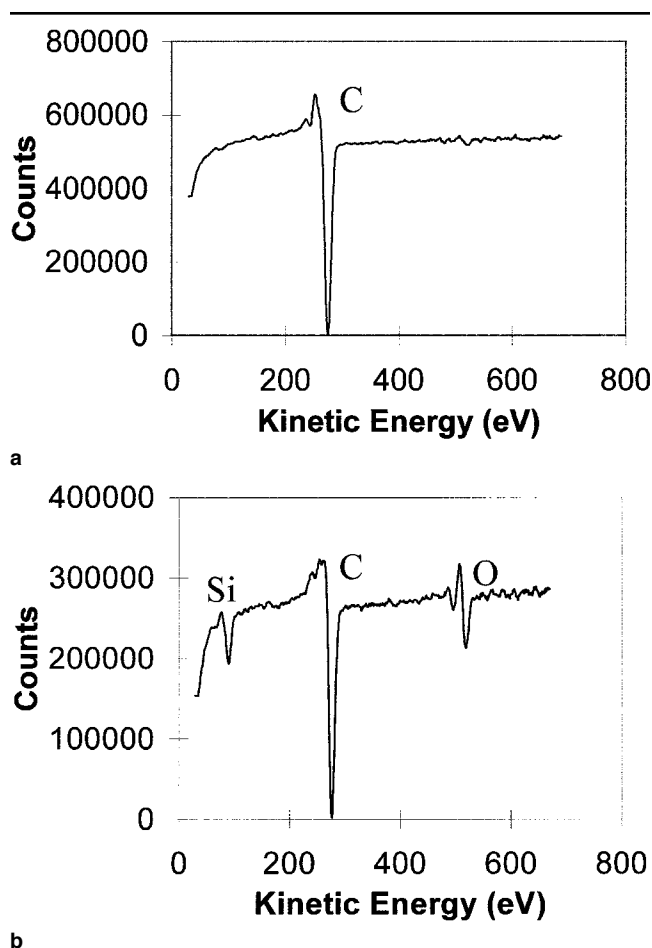


Fig. 5. Auger electron spectroscopy of the two regions on the cleaved SiC surface (a) inside a thermal decomposition cavity and (b) on the clean SiC surface.

form because of voids present in the attachment layer.

The inner surfaces of several cavities were inspected with SEM/EDX in order to determine their chemical makeup. Figure 4 is an SEM image of a tubular cavity, taken 4 mm from the seed/lid interface, and its corresponding EDX images for silicon and carbon. The sample shown was taken from a PVT grown SiC boule, which had been grown for 10 h (2300°C , gradient of $10^{\circ}\text{C}/\text{cm}$, argon pressure of 10 torr), and cleaved along the *c*-axis. The SEM image shows a tube intersecting the cleaved plane with a

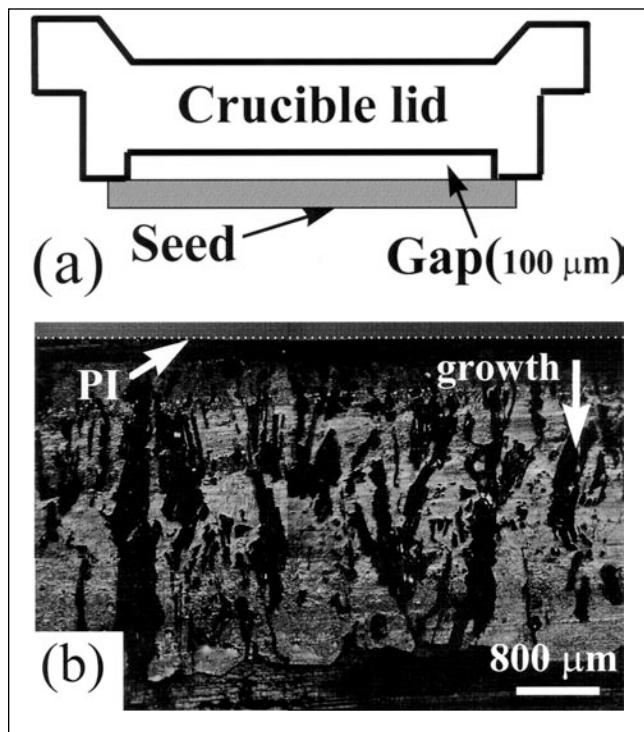
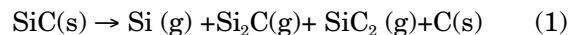


Fig. 6. (a) Schematic diagram of the mechanical mounting technique with an intentional gap. See text for experiment description. (b) Reflection optical micrograph of an axial slice of a crystal grown utilizing the mechanical mounting method, with an intentional gap (100 μm) behind the seed crystal. PI marks the interface between the polycrystalline SiC and the graphite lid.

diameter of approximately 5 μm and propagating along the growth direction. The high intensity in the carbon EDX image, represented by the bright areas, and low intensity in the silicon EDX image indicate that the cavity walls have a much higher carbon concentration and much lower silicon concentration than the SiC matrix. This result was additionally

supported by Auger spectroscopy on the same cleaved sample. Figure 5 shows two AES spectra; spectrum 5(a), taken on the inside wall of a tubular cavity, shows only the carbon peak. Spectrum 5(b), taken on the cleaved SiC boule surface indicates the presence of silicon, carbon and oxygen. A possible explanation for the higher concentration of carbon on the walls of the cavities is local sublimation of the SiC matrix. Under PVT growth conditions, SiC sublimates non-congruently, and releases mainly Si, Si₂C and SiC₂ as vapor species. Since the vapor is always silicon rich, the excess carbon is left behind,¹⁵ as shown in Eq. 1.



The volatile gases are then dissipated into the growth ambient, with solid carbon remaining inside the decomposition void.

The vapor transport in a standard PVT system is driven by an axial temperature gradient over the growth crucible. It is expected that the temperature gradient across voids in the carbonized attachment layer will lead to the transport of material from the hot seed to the cooler lid. However, in order for a long hollow tube to form, this transport must be efficient. The estimate of the transport rate was obtained in a growth experiment with an intentional gap between the seed crystal and the graphite lid. For this purpose the seed crystal was held mechanically, (Fig 2b), and a gap of approximately 100 μm was left between the seed and crucible lid, as illustrated in Fig. 6a. The growth experiment was carried out under the standard conditions (2300°C, 10°C/cm, 10 torr) for 1 h. Figure 6b is an optical image of a cross-sectional slice of the crystal after growth. The figure shows that the gap behind the seed has been filled with SiC containing many pores. It indicates that the entire seed has transported to the graphite lid as polycrystalline SiC, filling the gap that existed before the growth run. The

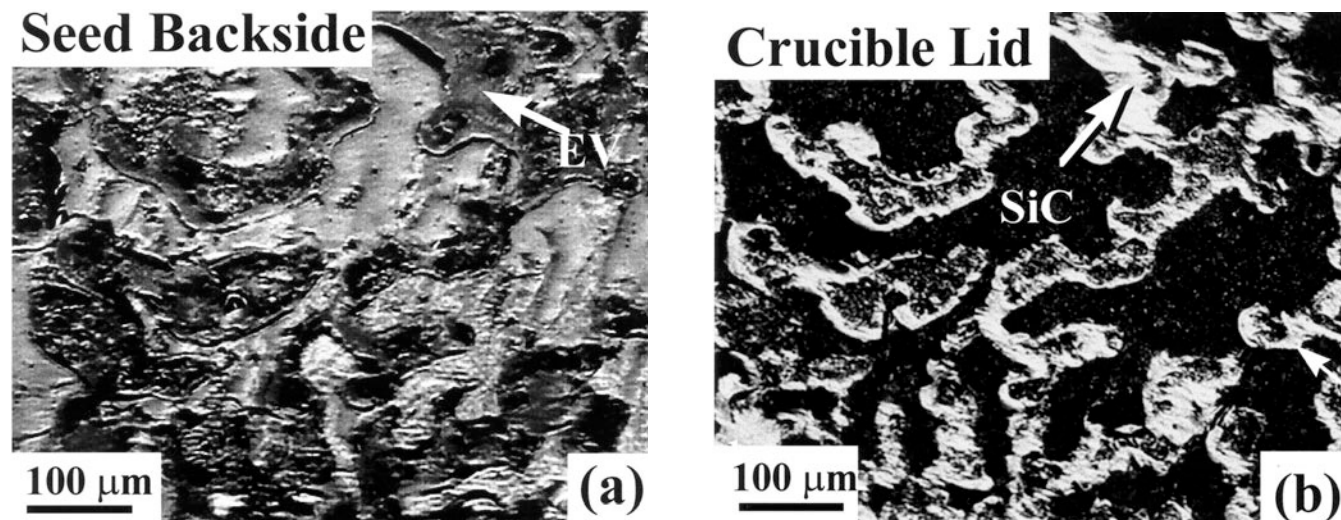


Fig. 7. Optical micrograph in reflected light of corresponding regions of the backside of a attached seed crystal (a) and the corresponding graphite lid (b). The image of the lid has been mirrored to allow for easier correlation of features. Dark regions in (a) are topographically lower than light regions. Dark regions in (b) are topographically lower than light regions. The arrow shows where SiC has been deposited on the lid directly under the evaporated region of the seed (marked with EV).

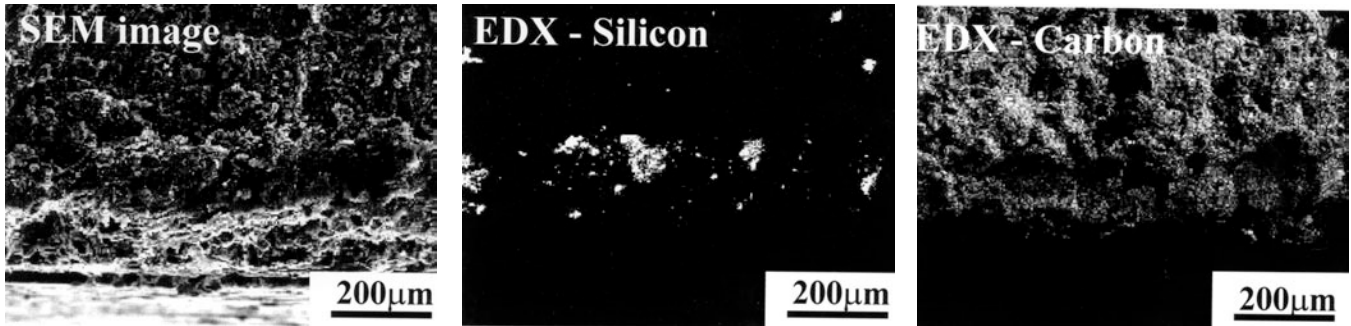


Fig. 8. Secondary electron and energy dispersive x-ray micrographs of the fractured graphite lid after growth. Note the degree of porosity in the graphite lid material and the presence of silicon in the porous graphite lid.

seed thickness before growth was 0.5 mm. Since the whole seed transported to the lid, the lower limit for the transport rate across the gap was 0.5 mm/h. This is on the same order of magnitude as the crystal growth rate in a standard PVT run.

A similar phenomenon of transport through voids was observed in glued seed crystals. A small Lely seed was mounted on the lid with sucrose, as described above. A growth experiment with the duration of 15 min was conducted at a temperature of 2300°C, with a gradient of 10 K/cm and an argon pressure of 10 torr. After the growth run the seed was removed from the crucible lid. Both the backside of the seed crystal and the mounting area of the lid were inspected with optical microscopy in reflected light. Figure 7a shows a section of the backside of the seed, and Fig. 7b, the corresponding area on the graphite crucible (mirrored). It is evident that there is a one to one relationship between the dark, topographically lower areas on the seed, and the bright, topographically higher areas on the cap. The crucible lid was further analyzed with powder x-ray diffraction. The resulting θ - 2θ scans had numerous peaks. Some were indexed as peaks from graphite while others were identified as due to SiC. Based on the above, the bright portions on the seed backside were interpreted as areas where the attachment layer created a bond between the lid and seed. The dark areas on the seed backside exhibit

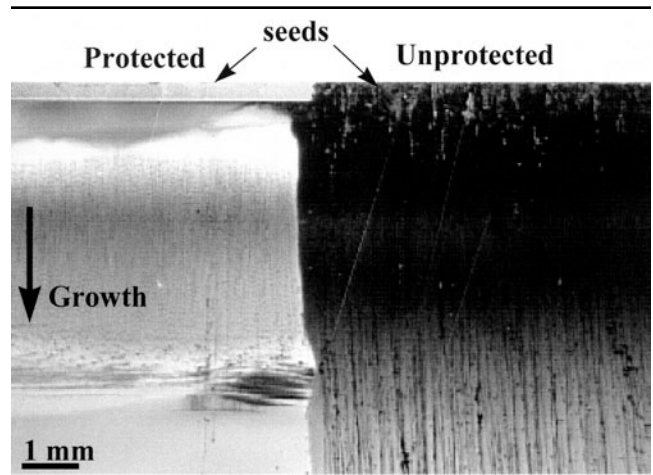


Fig. 9. Transmission optical microscopy image of a cross sectional slice along the [0001] growth direction of a dual seed growth at 2300°C for 14 h. The seed crystal on the left has been protected, by the application of a thin continuous film of graphite (carbonized photoresist) on the seed backside. Both seeds have been mounted on the same crucible lid using the sucrose attachment method.

marks of sublimation and correspond to the voids which existed in the attachment layer. In these locations the seed has locally sublimed, and the silicon carrying species have been transported across the void and deposited on the lid as SiC.

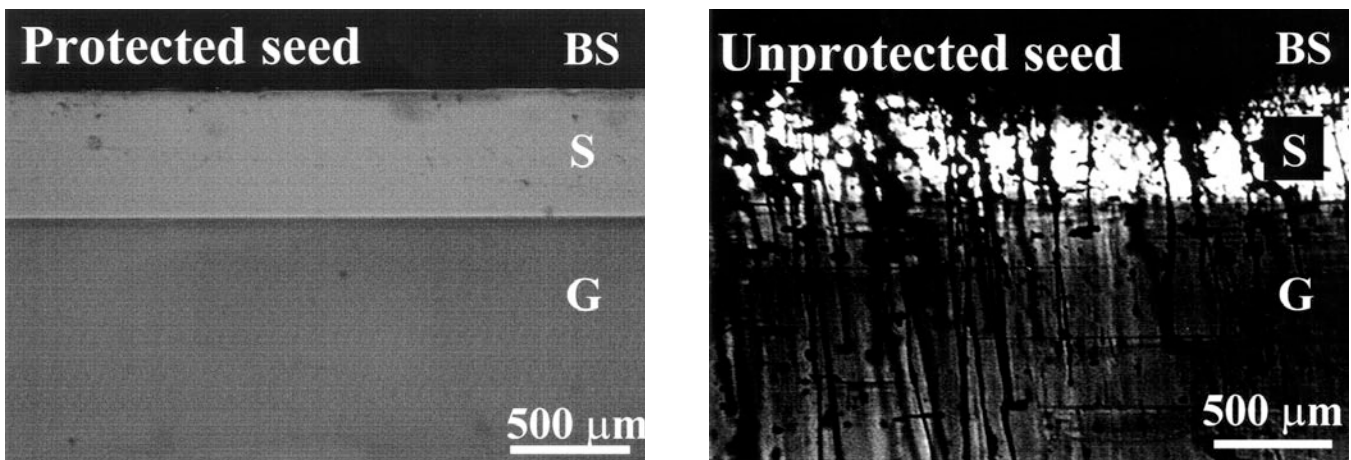


Fig. 10. Higher magnification optical cross-sectional images in transmitted light of the seed crystal/lid interfaces of the protected and the unprotected seed crystals shown in Fig. 9. BS marks the location of the seed backside, S is the Lely seed and G is the grown crystal.

In order for the proposed process to produce cavities, the silicon rich vapor has to be dissipated into the growth system. One possible mechanism for this process is the diffusion of silicon species through the porous graphite lid. In order to test this hypothesis, a SiC boule was removed from the crucible lid after growth. The graphite lid was then cleaved open and inspected with SEM/EDX. Figure 8 is a SEM image and its corresponding EDX images for silicon and carbon. The SEM image shows the fracture surface of the lid with the lid/seed interface at the bottom of Fig. 8a. As expected, the ATJ graphite lid contains pores. The EDX images indicate that the graphite lid contains silicon, up to 200 μm from the mounting surface. The intensity of the silicon signal is comparable to that of SiC.

The proposed formation mechanism of thermal decomposition cavities provides an insight to how their formation can be suppressed. The key to preventing them is to form a continuous diffusion barrier for silicon bearing species. To test this, a Lely platelet was cut into two parts. The backside of one seed crystal was painted with photoresist, approximately 15 μm thick, cured in a furnace at a temperature of 120°C for 5 min, and annealed in high vacuum ($< 3 \times 10^{-7}$ torr) at a temperature of 1200°C, utilizing a temperature ramp rate of 400°C/h. This procedure is similar to that used by Thomas et al.¹⁶ The resulting carbon protection layer was shiny and contained no visible cracks or voids. A seed crystal with the protection layer applied to its backside and an unprotected seed crystal were mounted side by side on the same crucible lid using the standard carbonized sucrose attachment layer. Both crystals were overgrown simultaneously in the same PVT growth experiment at a temperature of 2300°C, with gradient of 10 K/cm, under an argon pressure of 20 torr for 14 h. An axial slice parallel to the growth direction (c-axis) was cut from the boule revealing both seed crystals.

Figure 9 shows an optical microscope image of the slice in transmitted light. The protected seed crystal is transparent and shows no signs of backside decomposition while the unprotected seed crystal has thermal decomposition cavities propagating through the entire crystal. It is apparent that the continuous graphite film on the backside of the protected seed suppressed the non-uniform sublimation. Higher magnification images of both seeds are shown in Fig. 10. In the unprotected seed crystal (bottom image), thermal decomposition cavities originate at the seed/lid boundary between the seed and crucible lid. These features are not observed in the protected seed crystal. The protection layer eliminates the vapor diffusion path of Si. Silicon may still diffuse through the solid protective layer, however, this occurs at a rate which is much slower than the vapor transport and does not result in thermal decomposition cavities. It should also be mentioned that growth experiments conducted with a modified attachment technique that

yielded continuous carbonized sucrose layers, containing no observable voids, resulted in crystals with no thermal decomposition cavities. However, formation of the homogeneous attachment layer using carbonized sucrose is not entirely reproducible. These preliminary results suggest that a sufficiently continuous attachment layer can act as a protection layer.

CONCLUSIONS

A formation mechanism for the formation of thermal decomposition cavities during PVT growth of SiC is proposed based on experimental observations of the individual formation steps. Voids in the carbonized attachment layer between the backside of the SiC seed crystal and the mounting surface of the graphite lid cause local sublimation of the seed crystal. Energy dispersive x-ray analysis and Auger electron spectroscopy indicated that the walls of thermal decomposition cavities are decorated with a carbon-rich layer. The vapor was transported across the cavities along the axial temperature gradient applied to facilitate crystal growth. The vapor partially recrystallized on the exposed graphite surface of the lid, and partially diffused into the porous graphite material of the lid. A continuous, void-free carbon protection layer applied to the backside of the seed crystal helped to suppress the formation of thermal decomposition cavities at the interface between the seed crystal and the graphite lid.

REFERENCES

1. Yu.M. Tairov and V.F. Tsvetkov, *J. Cryst. Growth* 43, 209 (1978).
2. D.L. Barrett, R.G. Seidensticker, W. Gaida, R.H. Hopkins, and W.J. Choyke, *J. Cryst. Growth* 109, 17 (1991).
3. D.L. Barrett, J.P. McHugh, H.M. Hobgood, R.H. Hopkins, P.G. McMullin, R.C. Clarke, and W.J. Choyke, *J. Cryst. Growth* 128, 358 (1993).
4. H.M. Hobgood, D.L. Barrett, J.P. McHugh, R.C. Clarke, S. Sriram, A.A. Burk, J. Gregg, C.D. Brandt, R.H. Hopkins, and W.J. Choyke, *J. Cryst. Growth* 137, 181 (1994).
5. R.A. Stein, *Physica* 185b, 211 (1993).
6. Yu.A. Vodakov, A.D. Roenkov, M.G. Ramm, E.N. Mokhov, and Yu.N. Makarov, *Phys. Stat. Sol. (b)* 202, 177 (1997).
7. M. Anikin, M. Pons, K. Chourou, O. Chaix, J.M. Bluet, V. Lauer, and R. Madar, *Mater. Sci. Forum* 264-268, 45 (1998).
8. I. Khlebnikov, T.S. Sudarshan, V. Madangarli, and M.A. Capano, *Mater. Res. Soc. Symp. Proc.* 483, 123 (1998).
9. V.D. Heydemann, N. Schulze, D.L. Barrett, and G. Pensl, *Diamond and Related Materials* 6, 1262 (1997).
10. M. Dudley, S. Wang, W. Huang, C.H. Carter, Jr., V.F. Tsvetkov, and C. Fazi, *J. Phys. D: Appl. Phys.* 28, A63 (1995).
11. R.C. Glass, D. Henshall, V.F. Tsvetkov, and C.H. Carter, Jr., *Phys. Stat. Sol. (b)* 202, 149 (1997).
12. V. Balakrishna, R.H. Hopkins, G. Augustine, G.T. Dunne, and R.N. Thomas, *Inst. Phys. Conf. Ser.* 160, 321 (1997).
13. M. Tuominen, R. Yakimova, A. Vehanen, and E. Janzen, *Mater. Sci. Eng.* B57, 229 (1999).
14. J.A. Lely, *Ber. Dt. Ker. Ges.* 32, 229 (1955).
15. J. Drowart, G. De Maria, and M.G. Inghram, *J. Chem. Phys.* 29, 1015 (1958).
16. C. Thomas, C. Taylor, J. Griffen, M.G. Spencer, K. Kornegay, M. Capano, and S. Rendakova, *Spring MRS 1999 proceedings*, in print.